

A Hybrid Approach for Accurate Brain Tumor Detection Using Deep Learning Techniques

Saraf Anzum Shreya¹, Md. Abu Ismail Siddique², Antu Roy Chowdhury³ and Mst. Fateha Samad⁴

^{1,2,3,4} Electronics & Telecommunication Engineering

Rajshahi University of Engineering & Technology

Rajshahi, Bangladesh

Email: sasshreya2001@gmail.com, saif101303@gmail.com, anturoychowdhury3@gmail.com, fatehaeteruet@gmail.com

Abstract—Brain tumors are a major global health concern, contributing to many deaths each year. Early and accurate diagnosis is essential for improving patient outcomes. In this paper, we introduce a new hybrid approach for detecting brain tumors. We started by preprocessing MRI images—gray-scaling, enhancing contrast, and applying masking—to highlight important features. We then classified the images using five deep-learning techniques, and the custom VGG16 and VGG19 models performed better than the other models. Our study utilized a dataset of 7,023 images across four categories: Glioma, Meningioma, No-Tumor, and Pituitary tumors. The results from using VGG16 and VGG19 were impressive, achieving 97% accuracy, 97% precision, and a 97% F1 score. These findings underscore the potential of our approach to enhance diagnostic accuracy and ultimately improve patient care.

Index Terms—Brain Tumor, VGG16, VGG19, ResNet50, DenseNet121, Xception, Deep Learning, and Computer Vision.

I. INTRODUCTION

The abnormal growth of cells in the brain leads to the development of brain tumors. These tumors known as primary brain tumors that is developed in the brain. It becomes secondary tumors when spread to other parts of the body. In 2019, there were approximately 348,000 new cases of brain tumors worldwide, with 187,000 leading to death [1].

Brain tumors are typically divided into two categories: malignant (cancerous) and non-malignant (non-cancerous). Non-malignant tumors are less aggressive, whereas malignant tumors, like Glioblastomas, are more severe and dangerous. Glioblastoma is a type of Glioma that is the most common and aggressive form of malignant brain tumor, making up around 14.5% of all brain tumors. It develops from glial cells, which help support and protect neurons [2]. On the other hand, Meningiomas are the most common type of non-malignant brain tumor, accounting for about 38.3% of cases [3]. These tumors originate in the meninges, the membranes surrounding the brain and spinal cord. Pituitary tumors form in the pituitary gland at the base of the brain, which plays a critical role in regulating hormone-related functions [4].

Traditional diagnosis of brain tumors involves a mix of clinical evaluations and imaging techniques like CT and MRI scans, and sometimes biopsies. However, these methods can take days to provide a clear diagnosis. This process has become much faster and more accurate thanks to advancements

in artificial intelligence (AI) and machine learning (ML). These technologies enable quicker diagnoses and can help with early detection, making treatment more effective [5].

In this study, we explored the use of machine learning for brain tumor detection. We trained several pre-existing deep learning models with customized additional layers, on a publicly available brain tumor dataset [6]. This dataset includes four categories: Glioma, Meningioma, Pituitary tumors, and a no-tumor class. Out of the models tested, both of the custom models, VGG16 and VGG19 have achieved the highest accuracy, reaching 97%.

II. LITERATURE REVIEW

As brain tumors have become a life-threatening problem, the diagnosis of it has not become as efficient or fast. Traditionally, the diagnosis of brain tumors depends on the manual analysis of MRI images and CT scans which is a time-consuming process and prone to human error. As machine learning has proved to be more precise and accurate, the use of it in this field has helped overcome these shortcomings.

In an article, Kushwaha et. al [7], trained a convolutional neural network (CNN) model on a dataset with 1200 MRI images of tumors and 1000 images of no-tumors. The model was able to successfully detect MRI images with tumors from no-tumor images. It had a high accuracy of 96%, a precision of 96.73% and the F1-score of the model was 95.54%. Although the model was successfully able to detect brain tumors, it was not able to specify brain tumors.

Sivadas et. al [8] have used convolutional neural network (CNN) features with support vector machine (SVM) in the model. This model was trained on MRI images of three types of brain tumors. The purpose of the paper was to use CNN feature selection with SVM classifier to attain high accuracy, which was 95.82%.

In another paper, Gayathiri et. al [9] proposed a Convolutional stacked Autoencoder Network (C-SAN) for brain tumor detection from MRI images. The dataset is processed through (NLM) filter. Then the filtered images were segmented by V-Net. After doing feature detection brain tumor detection was performed by C-SAN, which was devised by integrating Convolutional Neural Network (CNN) and Deep Stacked Autoencoder (DSAE). This model attained an accuracy of 0.909 and a sensitivity of 0.958.

Loganayagi et. al [10] proposed a model that used the Gray Level Co-occurrence Matrix (GLCM) and the Entropy-based GDP (EGDP) to extract features. It was applied to an augmented brain tumor dataset. On the extracted features, the deep convolutional belief network (DCvB-Net) was trained and was able to attain an accuracy of 92.3%.

After that Ullah et. al [11] proposed a hybrid model with ResNet50 with the combination of Gabor feature and SVM classification. This model was able to achieve an accuracy of 95.73%, 95.90% and 95.72% in precision and f1 score. However, they have some computation limitations in their research.

In our study, we preprocessed the images of a public dataset followed by masking those images to extract the focused area to detect tumors. We trained 5 models with custom layers. Among these models, the custom VGG16 and VGG19 models both had the best result with a test accuracy of 96.57%, an overall accuracy of 97%, and 97% in both F1-score and precision. Our model performs better than other existing model for this work.

III. MATERIALS & METHODS

A. Research Roadmap

Figure 1 showcases the entire research process in that we begin with the data preprocessing. Later on, we masked the dataset then we split the data set into three regions train, validation, and test dataset. After that go through with the deep learning model and find out the performance matrix.

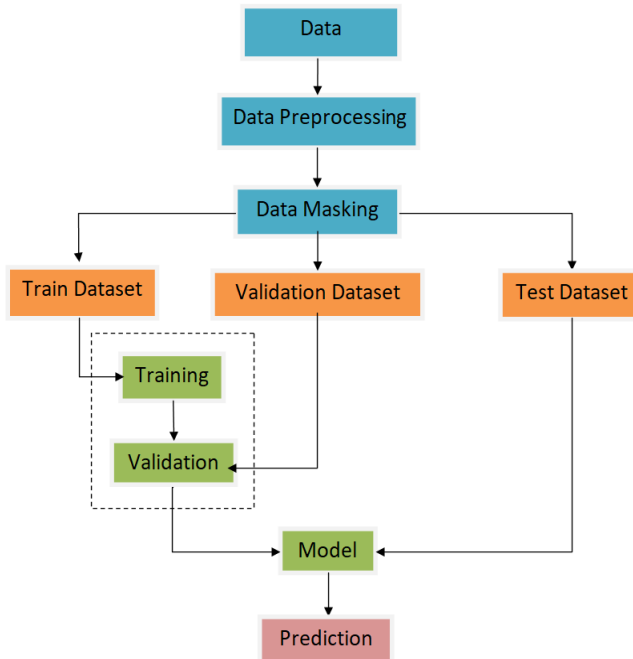


Fig. 1: Proposed Roadmap for Brain Tumor Detection

B. Data Acquisition

In this study, a public dataset from Kaggle was used to train our models, which was already divided into train and test

datasets. This dataset is a combination of these three datasets: figshare, SARTAJ dataset, and Br35H. It contains 7023 images of human brain MRI images [6], having 4 classes: glioma, meningioma, no tumor, and pituitary.

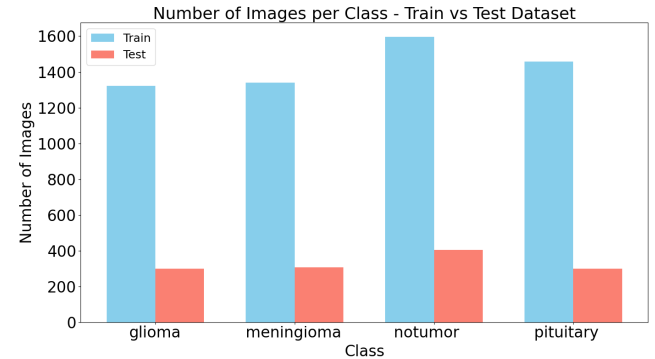


Fig. 2: Distribution of Data in the Training and Testing Sets
C. Data Preprocessing

The images from the dataset were resized to 256x256 pixels for consistency. They were then converted to grayscale to make processing easier. Next, the contrast was increased to highlight the tumor areas, and masking was applied to focus on these regions for further analysis 4. Figure 3 demonstrates the data preprocessing procedures.



Fig. 3: Data Preprocessing Steps

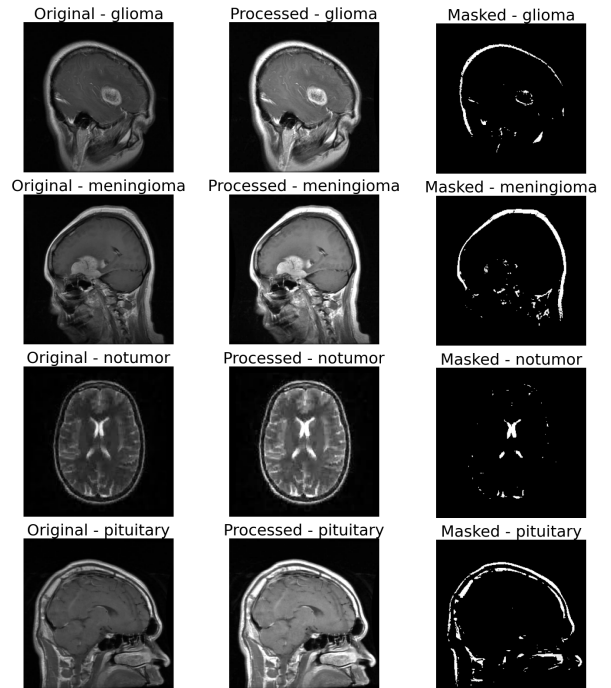


Fig. 4: Example of Processed Image Data

D. Base Models with Custom Layers

In our study, five popular deep learning architectures were trained for the detection of brain tumors: ResNet50, Xception, DenseNet121, VGG19, and VGG16. These models were extended with custom layers to fine-tune them and prepare them for detection.

1) *ResNet50*: ResNet50, developed by a team of researchers from Microsoft Research is a deep convolutional neural network (CNN) that is widely used in medical imaging for detecting various diseases like cancer, tumors, and other conditions. This ResNet50 model has processed the input and outputs a feature map with dimensions of (None, 8, 8, 2048). A more detailed architecture of this model is shown in Table [I]

TABLE I: ResNet50 Model Architecture Summary

Layers	Output Shape	Parameters
Input	(None, 256, 256, 1)	0
ResNet50	(None, 8, 8, 2048)	23,581,440
Conv2D	(None, 8, 8, 512)	9,437,696
Conv2D	(None, 8, 8, 512)	2,359,808
Batch Normalization	(None, 8, 8, 512)	2,048
MaxPooling2D	(None, 4, 4, 512)	0
Flatten	(None, 8192)	0
Dense	(None, 128)	1,048,704
Batch Normalization	(None, 128)	512
Dropout	(None, 128)	0
Dense	(None, 4)	516
Trainable	36,376,324 (138.76 MB)	
Non-trainable	54,400 (212.50 KB)	

2) *Xception*: Xception also known as Extreme Inception, is a powerful deep learning model. It is based on the principle of depthwise separable convolutions, making it suitable for tasks like identifying abnormalities in MRI scan. The details about the model's architecture are shown in Table [II].

TABLE II: Xception Model Architecture Summary

Layers	Output Shape	Parameters
Input	(None, 256, 256, 1)	0
Xception	(None, 8, 8, 2048)	20,860,904
Conv2D	(None, 8, 8, 512)	9,437,696
Conv2D	(None, 8, 8, 512)	2,359,808
Batch Normalization	(None, 8, 8, 512)	2,048
MaxPooling2D	(None, 4, 4, 512)	0
Flatten	(None, 8192)	0
Dense	(None, 128)	1,048,704
Batch Normalization	(None, 128)	512
Dropout	(None, 128)	0
Dense	(None, 4)	516
Trainable	33,654,380 (128.38 MB)	
Non-trainable	55,808 (218.00 KB)	

3) *DenseNet121*: DenseNet121 is a robust deep learning model designed for image classification. Its architecture uses dense connections between layers, enhancing its performance on complex tasks like identifying tumors in MRI scans. The details of the custom DenseNet121 model architecture are summarized in Table [III].

TABLE III: DenseNet121 Model Architecture Summary

Layers	Output Shape	Parameters
Input	(None, 256, 256, 1)	0
DenseNet121	(None, 8, 8, 2048)	7,031,232
Conv2D	(None, 8, 8, 512)	4,719,104
Conv2D	(None, 8, 8, 512)	2,359,808
Batch Normalization	(None, 8, 8, 512)	2,048
MaxPooling2D	(None, 4, 4, 512)	0
Flatten	(None, 8192)	0
Dense	(None, 128)	1,048,704
Batch Normalization	(None, 128)	512
Dropout	(None, 128)	0
Dense	(None, 4)	516
Trainable	15,076,996 (57.51 MB)	
Non-trainable	84,928 (331.75 KB)	

4) *VGG19*: VGG19 is another widely used deep learning model known for its simplicity and effectiveness in image classification, including medical imaging applications. The architecture of the custom VGG19 model is presented in Table [IV].

TABLE IV: VGG19 Model Architecture Summary

Layers	Output Shape	Parameters
Input	(None, 256, 256, 1)	0
VGG19	(None, 8, 8, 512)	20,023,232
Conv2D	(None, 8, 8, 512)	2,359,808
Conv2D	(None, 8, 8, 512)	2,359,808
Batch Normalization	(None, 8, 8, 512)	2,048
MaxPooling2D	(None, 4, 4, 512)	0
Flatten	(None, 8192)	0
Dense	(None, 128)	1,048,704
Batch Normalization	(None, 128)	512
Dropout	(None, 128)	0
Dense	(None, 4)	516
Trainable	25,793,348 (98.39 MB)	
Non-trainable	1,280 (5.00 KB)	

5) *VGG16*: VGG16 is a deep learning model developed by the Visual Geometry Group [12] known for its simple yet powerful architecture. It is often used for image classification tasks, including medical imaging for disease detection. In this model, 13 trainable models were used along with a few custom layers. More details are shown in the table [V]

TABLE V: VGG16 Model Architecture Summary

Layers	Output Shape	Parameters
Input	(None, 256, 256, 1)	0
VGG16	(None, 8, 8, 512)	14,713,536
Conv2D	(None, 8, 8, 512)	2,359,808
Conv2D	(None, 8, 8, 512)	2,359,808
Batch Normalization	(None, 8, 8, 512)	2,048
MaxPooling2D	(None, 4, 4, 512)	0
Flatten	(None, 8192)	0
Dense	(None, 128)	1,048,704
Batch Normalization	(None, 128)	512
Dropout	(None, 128)	0
Dense	(None, 4)	516
Trainable	20,483,652 (78.14 MB)	
Non-trainable	1,280 (5.00 KB)	

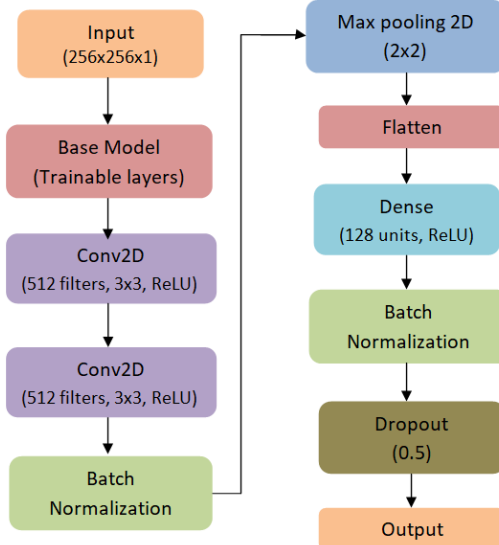


Fig. 5: Diagram of Custom Model

E. Evaluation Metrics

We focused on key metrics such as accuracy, precision, recall, F1-score, and ROC curves. Accuracy gives an overall sense of how well the model performs in predicting correctly. Precision shows how good the model is at avoiding false positives, while recall (or sensitivity) tells us how well it identifies the correct cases. The F1-score balances precision and recall for a more rounded view of the model's performance, especially in situations with imbalanced classes or when false positives and false negatives are equally important [13]. Finally, the ROC curve helps visualize the trade-off between true positives and false positives, making it useful for analyzing different decision thresholds.

Equations (1), (2), (3), and (4) represent the calculations for Accuracy, Precision, Recall, and F1 Score, respectively.

$$\text{Accuracy} = \frac{\text{TP} + \text{TN}}{\text{TP} + \text{TN} + \text{FP} + \text{FN}} \quad (1)$$

$$\text{Precision} = \frac{\text{TP}}{\text{TP} + \text{FP}} \quad (2)$$

$$\text{Recall (Sensitivity or TPR)} = \frac{\text{TP}}{\text{TP} + \text{FN}} \quad (3)$$

$$\text{F1 Score} = \frac{2 \times \text{Precision} \times \text{Recall}}{\text{Precision} + \text{Recall}} \quad (4)$$

Where, TP: True Positive, FP: False Positive, TN: True Negative, FN: False Negative.

IV. RESULT & ANALYSIS

In this section, we thoroughly analyze the performance metrics and effectiveness of all of our models.

A. ROC Curves & Confusion Matrices

The ROC (Receiver Operating Characteristic) curve is a graphical representation of a classifier's performance, plotting the true positive rate against the false positive rate at various threshold settings. The AUC (Area Under the Curve) quantifies the overall ability of the model to distinguish between classes.

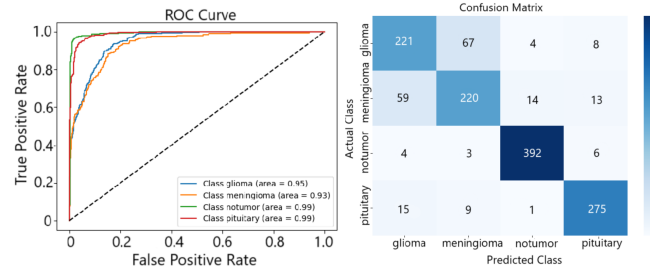


Fig. 6: ResNet50 ROC Curve & Confusion Matrix

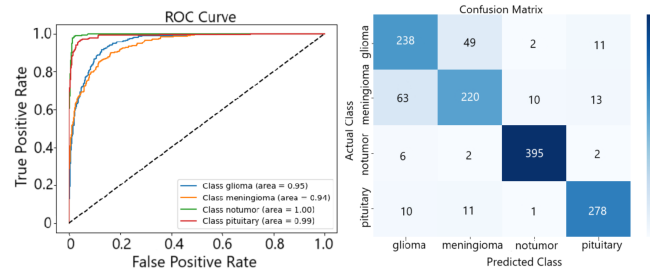


Fig. 7: Xception ROC Curve & Confusion Matrix

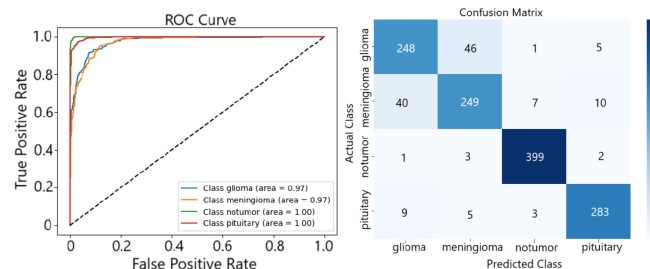


Fig. 8: DenseNet121 ROC Curve & Confusion Matrix

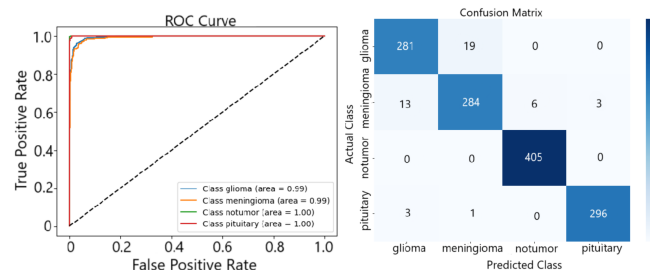


Fig. 9: VGG19 ROC Curve & Confusion Matrix

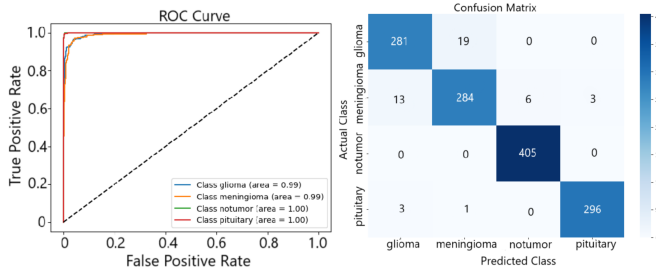


Fig. 10: VGG16 ROC Curve & Confusion Matrix

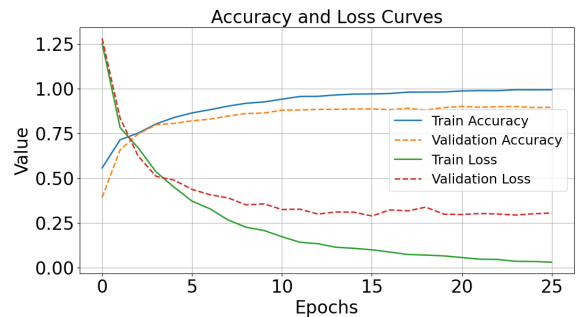


Fig. 13: DenseNet121 Accuracy & Loss Curve

B. Accuracy and Loss Curves

We monitored five of our model's performances using the accuracy and loss curves depicted in Figure ??.

All of our models consistently improved their training and validation accuracy as the training advanced. To ensure fairness, we kept hyperparameters and epoch counts standardized. VGG16, VGG19 and DenseNet121 achieved their peak performance after 20 epochs, whereas Xception reached its peak after 5 and ResNet50 at 35 epochs.

We used callbacks, early stopping, reduce lr and model checkpoints, employed the Adam optimizer, and utilized categorical crossentropy loss with a constant batch size of 32.

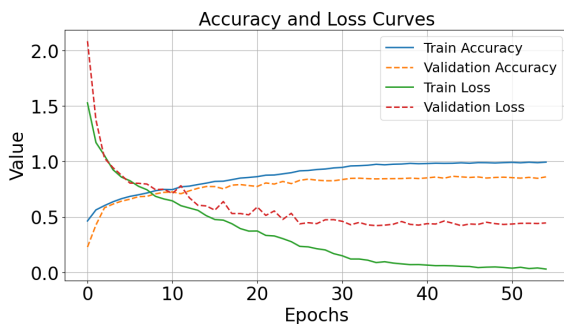


Fig. 11: ResNet50 Accuracy & Loss Curve

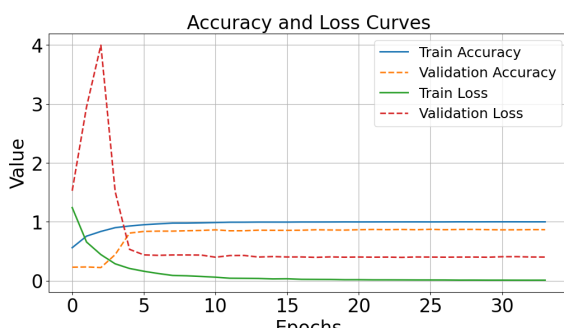


Fig. 12: Xception Accuracy & Loss Curve

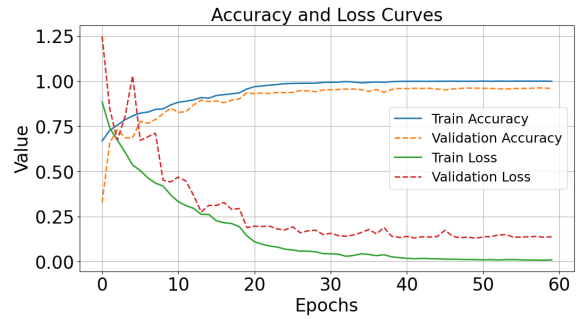


Fig. 14: VGG19 Accuracy & Loss Curve

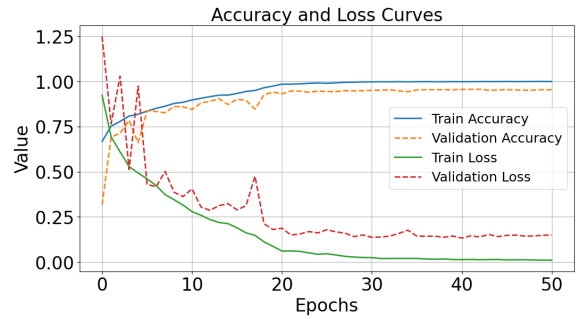


Fig. 15: VGG16 Accuracy & Loss Curve

C. Performance Metrics Evaluation

We evaluated the effectiveness of each model by analyzing key metrics such as precision, recall, and F1-score, as presented in Table VI. Our custom VGG16 and VGG19 models achieved an impressive accuracy of 97%. VGG19 demonstrated slightly better recall, achieving 94%, which is 2% higher than VGG16. However, VGG16 surpassed VGG19 in terms of precision, attaining 96%, which is 1% higher. These differences indicate that VGG16 may be more reliable in correctly identifying positive cases, while VGG19 has a slight edge in ensuring that fewer relevant instances are missed.

Table VI displays the performance metrics of each model. Custom VGG16 and VGG19 exhibit impressive accuracy of 97%. VGG19 outperforms VGG16 in recall with 94% by 2%. But VGG16 outperforms VGG19 in precision with 96% by 1%.

Metric	Model Name	glioma	meningioma	notumor	pituitary
Precision	ResNet50	0.75	0.78	0.97	0.91
	Xception	0.75	0.78	0.97	0.91
	DenseNet121	0.83	0.82	0.97	0.94
	VGG19	0.95	0.93	0.99	0.99
	VGG16	0.96	0.93	0.99	0.99
Recall	ResNet50	0.77	0.73	0.97	0.93
	Xception	0.79	0.72	0.98	0.93
	DenseNet121	0.83	0.81	0.99	0.94
	VGG19	0.94	0.93	1.00	0.99
	VGG16	0.92	0.93	1.00	0.99
F1-score	ResNet50	0.76	0.75	0.97	0.92
	Xception	0.77	0.75	0.97	0.92
	DenseNet121	0.83	0.82	0.98	0.94
	VGG19	0.94	0.93	0.99	0.99
	VGG16	0.94	0.93	0.99	0.99

TABLE VI: Performance comparison of different models across various metrics and classes

D. Comparison with Recent Studies

Table VII summarizes our achievements in brain tumor detection, comparing our results to existing methods. It highlights the competitive performance of traditional and hybrid deep learning models. While older models such as CNN and CNN + SVM from 2021 and 2024 achieved accuracies between 95.82% and 96%, our custom VGG19 and VGG16 models reached 97%, outperforming these earlier approaches. Recent models like DCvB-Net + EGDP and C-SAN + V-net show promise with their respective accuracies of 92.3% and 90.9%. However, despite their innovative structures, they still fall short of the performance levels achieved by VGG19 and VGG16 in our work.

TABLE VII: Comparative Works of Brain Tumor Detection Models

Ref	Year	Model	Dataset	Acc (%)
[7]	2024	CNN	Kaggle	96%
[8]	2021	CNN + SVM	Figshare	95.82%
[9]	2025	C-SAN + V-net	-	90.9%
[10]	2024	DCvB-Net + EGDP	-	92.3%
[11]	2023	ResNet50 + Gabor	figshare SARTAJ dataset Br35H	95.73%
Our Work	2024	ResNet50 Xception DenseNet121 VGG19 VGG16	figshare SARTAJ dataset Br35H	86% 87% 90% 97% 97%

V. CONCLUSION & DISCUSSION

In our study, we assessed five widely-used deep learning models—ResNet50, Xception, DenseNet121, VGG19, and VGG16 with custom layers—for detecting brain tumors. We tracked the performance of each model over multiple epochs by analyzing metrics such as accuracy, loss, and ROC curves, ensuring fairness by standardizing hyperparameters and maintaining consistent batch sizes during training. VGG16 and VGG19 also excelled in precision, recall, and F1-score. While

VGG19 slightly surpassed VGG16 in recall (94% vs. 92%), VGG16 had a marginal advantage in precision (96% vs. 95%), demonstrating that both models are highly reliable for brain tumor classification. However, VGG19's higher recall makes it more effective in detecting all true positives. Callbacks such as early stopping and learning rate reduction were crucial for stabilizing training and improving performance. In summary, VGG19 and VGG16 emerged as the top models for brain tumor detection, both achieving 97% accuracy, with VGG19 excelling in recall and VGG16 in precision, making them highly effective for medical imaging tasks. This model not only detects brain tumors but also can be used to classify other images.

REFERENCES

- [1] M. I. Irena Illic, "International patterns and trends in the brain cancer incidence and mortality: An observational study based on the global burden of disease," *Heliyon*, vol. 9, no. 7, July 2023.
- [2] A. B. T. Association, "Glioblastoma facts statistics," 2020. Available: <https://www.abta.org>.
- [3] G. C. K. W. C. K. J. S. B.-S. Quinn T Ostrom, Nirav Patil, "Cbrus statistical report: Primary brain and other central nervous system tumors diagnosed in the united states in 2013–2017," *Neuro-Oncology*, vol. 22, no. 1, p. 2, 2020.
- [4] C. T. C. of America, "Pituitary tumors facts and overview," 2021. Available: <https://www.cancercenter.com>.
- [5] A. Esteva, A. Robicquet, B. Ramsundar, V. Kuleshov, M. DePristo, K. Chou, C. Cui, G. S. Corrado, S. Thrun, and J. Dean, "A guide to deep learning in healthcare," *Nature medicine*, vol. 25, no. 1, pp. 24–29, 2019.
- [6] M. Nickparvar, "Brain tumor mri dataset," 2021. <https://www.kaggle.com/dsv/2645886>.
- [7] P. K. Kushwaha, A. Rana, B. P. Lohani, A. Gupta, C. Laishram, and K. Ayyasamy, "Brain tumour detection using mri images and cnn architecture," in *2024 International Conference on Communication, Computer Sciences and Engineering (IC3SE)*, pp. 540–548, 2024.
- [8] D. Sivadas and P. Ameer, "Automated categorization of brain tumor from mri using cnn features and svm," *Journal of Ambient Intelligence and Humanized Computing*, vol. 12, pp. 1–13, 08 2021.
- [9] R. Gayathiri and S. Santhanam, "C-san: Convolutional stacked autoencoder network for brain tumor detection using mri," *Biomedical Signal Processing and Control*, vol. 99, p. 106816, 2025.
- [10] G. R. Loganayagi T, Pooja Panapana and S. Das, "Egdp based feature extraction and deep convolutional belief network for brain tumor detection using mri image," *Network: Computation in Neural Systems*, vol. 0, no. 0, pp. 1–31, 2024. PMID: 39285629.
- [11] S. Ullah, M. Ahmad, S. Anwar, and M. Khattak, "An intelligent hybrid approach for brain tumor detection," *Pakistan Journal of Engineering and Technology*, vol. 6, pp. 42–50, 02 2023.
- [12] K. Simonyan and A. Zisserman, "Very deep convolutional networks for large-scale image recognition," *arXiv preprint arXiv:1409.1556*, 2014.
- [13] C. D. Manning, P. Raghavan, and H. Schütze, *Introduction to Information Retrieval*. Cambridge University Press, 2008.